Results in Physics 38 (2022) 105619

Contents lists available at ScienceDirect

Results in Physics

journal homepage: www.elsevier.com/locate/rinp

Robust thermal correlations induced by spin–orbit interactions

Ahmad N. Khedr [a], Ali H. Homid [b], Abdel-Baset A. Mohamed [c,d], Abdel-Haleem Abdel-Aty [a,e,*], Hichem Eleuch [f,g,h], Mahmoud Tammam [a], Mahmoud Abdel-Aty [i]

[a] Physics Department, Faculty of Science, Al-Azhar University, Assiut 71524, Egypt
[b] Mathematics Department, Faculty of Science, Al-Azhar University, Assiut 71524, Egypt
[c] Mathematics Department, College of Science and Humanities in Al-Aflaj, Prince Sattam bin Abdulaziz University, Saudi Arabia
[d] Department of Mathematics, Faculty of Science, Assiut University, Assiut 71515, Egypt
[e] Department of Physics, College of Sciences, University of Bisha, PO Box 344, Bisha 61922, Saudi Arabia
[f] Department of Applied Physics and Astronomy, University of Sharjah, Sharjah, United Arab Emirates
[g] College of Arts and Sciences, Abu Dhabi University, Abu Dhabi 59911, United Arab Emirates
[h] Institute for Quantum Science and Engineering, Texas A&M University, College Station, TX 77843, USA
[i] Mathematics Department, Faculty of Sciences, Sohag University, Sohag, Egypt

A R T I C L E I N F O

Keywords:
Nonclassical correlations
Heisenberg XYZ two-spin system
Spin–orbit interaction
Equilibrium temperature

A B S T R A C T

In this work, we demonstrate that the thermal nonclassical correlations can enhance and become more stable under the magnetic field and second-order spin–orbit interaction effect. Also, we show that the local quantum uncertainty measure can reveal purely quantum correlations beyond other quantifiers of correlations. Our analytical model describes a Heisenberg XYZ two-spin system with an inhomogeneous magnetic field and spin–orbit interaction. A special emphasis is devoted to local quantum uncertainty, concurrence, and Bell-nonlocality measures to investigate the correlations of the bipartite-system at the equilibrium temperature. Our results indicate that temperature, magnetic field, and magnetic field inhomogeneity with DMI and Kaplan–Shekhtman–Entin-Wohlman–Aharony (KSEA) exchanges all play a role in determining the degree of correlation between the quantum spins to some extent. The KSEA interaction greatly enhances the quantum correlation in the system whereas quantum quantifiers are more stable under the influence of the external magnetic field, especially when inhomogeneous and homogeneous magnetic field are near to zero. Furthermore, these findings suggest that the thermal LQU captures a stronger quantum correlation than the Bell-nonlocality and entanglement measures.

Introduction

During the last decade, tremendous progress has been made in the investigation of quantum correlations (QCs) beyond entanglement. QCs are already common in many natural systems, and they play an important role in quantum computing technology due to their high technical potential [1]. The QCs preservation is one of the most challenging problems for the quantum technology [2–4]. The Einstein–Podolsky–Rosen (EPR) [5,6] pique interest in the entanglement phenomenon, which has stirred up a long-running discussion about quantum theory vs classical theory. Entanglement is a kind of QC that may be quantified in several ways, such as negativity and concurrence [7].

On the other hand, quantum non-locality, such as that indicated by the Bell inequalities violation by quantum entangled states [6], is one of the more practical ways of startling predictions of quantum mechanics. Recently, as confirmed in loophole-free experiments [8–10]. Bell-type inequalities [11] are a popular way to measure non-locality. Now, the non-classical correlations and non-locality including quantum entanglement were considered features of QCs. Furthermore, the concept of quantum correlations qualifies to perform numerous quantum information processing tasks that are not classically achievable [12–14]. The resources of non-classical correlations can be exploited for enhancing ways of transmitting and manipulating information, such as quantum dense coding [15], entanglement swapping [16], quantum key distribution [17], quantum computing and quantum cryptography [18]. Also quantum non-locality has been proven to be useful in many quantum tasks, such as machine learning techniques to network nonlocality [19] and randomness certification [20].

Indeed, a new categorization system for correlations based on quantum measurement techniques has emerged, and it plays a major role in quantum information theory. In particular, to measure this quantum correlation, quantum discord (QD) [21] is used as another type of non-local correlation. Meanwhile, there are separable cases with non-zero

* Corresponding author at: Department of Physics, College of Sciences, University of Bisha, PO Box 344, Bisha 61922, Saudi Arabia.
E-mail address: amabdelaty@ub.edu.sa (A.-H. Abdel-Aty).

https://doi.org/10.1016/j.rinp.2022.105619
Received 28 February 2022; Received in revised form 2 May 2022; Accepted 13 May 2022
Available online 21 May 2022

discord that can be employed to accomplish beneficial quantum processes [22,23]. Obtaining a mathematical technique for determining quantum discord, on the other hand, is only conceivable in a few rare situations, and the general case is rather difficult [24].

To avoid these issues, the local quantum uncertainty (LQU) technique was suggested as the principal quantifier for determining non-classical correlations [25]. Furthermore, unlike the other measures, this reliable quantifier meets all the conditions for quantum correlation measurements and is easy to compute. This measure, which is based on the lower bound of the skew information [26] over all feasible local measurements, has sparked considerable attention and has been thoroughly investigated [27–29]. It is also connected to Fisher's quantum information, making it a helpful resource in quantum metrology [30,31].

Spin chain systems have recently emerged as viable possibilities for establishing non-classical correlation because they possess several distinguishing characteristics when compared to other physical systems [32,33]. They are responsible for carrying data based on quantum correlations. [34]. Besides, the conventional materials of atoms can incorporate various types of interactions, like spin–spin interaction and spin–orbit interaction (SOI) that are specified by multiferroic mechanisms [35]. The SOI emerges as a result of the presence of structural inversion asymmetry within the materials, causing anisotropic exchange coupling between the spins. A Heisenberg model, which has been simplified to an Ising model, describes such an SOI [36]. Moreover, Heisenberg spin chains have piqued the interest of many researchers because of their importance in the modeling and simulation of several systems, including qubits based on quantum annealing processes [2,37], quantum dots, electronic spin, and optical lattices [38,39], providing potential applications to quantum computing (see Ref. [2,40]). The dynamics of this system can be simulated on the IBM quantum computer [41].

In addition, the SOI can generate two types of anisotropy one called Dzyaloshinskii–Moriya interaction (DMI) effect [42] and other called Kaplan–Shekhtman–Entin-Wohlman–Aharony (KSEA) effect [43]. The KSEA interaction has been observed experimentally in the helimagnetic insulator $Ba_2CuGe_2O_7$ [44]. These effects are significant in quantum information and KSEA effect can compensate the destruction of SU(2) symmetry by DMI. Furthermore, the DMI and KSEA effects play an important role in modulating the dynamic properties of quantum correlations as it can overcome the local minimum of non-classical correlation [45]. In this context, there has recently been a growing interest in the quantification and description of quantum correlations in various models of the two-qubit Heisenberg spin-chain [37,46]. Experimentally, thermal entanglement in a spin chain formed by the combination $Na_2Cu_5Si_4O_{14}$ has been observed [47]. The features of the spin chain model with the Dzyaloshinskii–Moriya (DM) exchange (arising from spinorbit coupling) in particular have been extensively investigated, which can induce another type of anisotropy. Entanglement and quantum discord measurements in bipartite systems in the XYZ Heisenberg spin models with DMI and KSEA have also been examined [48–50].

Motivated by the aforementioned studies, we investigate the combined influences of the DMI and KSEA exchanges in non-classical correlation in the Heisenberg model, which are frequently ignored in several works but may have a significant impact on the dynamical properties of quantum systems. The establishment of an appropriate quantifier for non-classical correlations in hybrid quantum systems, is crucial. Moreover, the effect of temperature and magnetic field on quantum correlations properties prompts the system to various types of dynamics, such that sudden death of the quantum correlations. Some studies [51,52] have investigated the thermal behavior of QC without considering the influence of DMI (antisymmetric) and KSEA (symmetric) effects in the case of thermal equilibrium. In this regard, we present a comparative investigation of the distinct pairwise thermal quantum correlation quantifiers in a two-qubit anisotropic Heisenberg XYZ spin-1/2 chain system under the effects of DMI and KSEA interactions, as well as the effects of a transverse uniform (non-uniform) magnetic field in this article. The influences of temperature and coupling interactions in a specific direction with DMI and KSEA interactions on quantum correlation measurements are thoroughly examined and discussed. Further, the local quantum uncertainty, Bell-non locality and entanglement measures are employed to quantify the impact of spin symmetry on thermal non-classical correlations. Also, we illustrate the behavior of QC in the presence of DMI and KSEA interactions and external magnetic fields.

The outline of the manuscript is as follows: In Section "Physical model and its thermal equilibrium", we introduce the Hamiltonian model and its thermal equilibrium. In Section "Nonclassical correlation measures", we present the non-classical correlations measures. We discuss the results in Section "Results and Discussion". Section "Conclusions" concludes our findings.

Physical model and its thermal equilibrium

Heisenberg spin chains are useful approaches in quantum information applications because they illustrate non-classical correlations and entanglement phenomena. In the late 1920's, Heisenberg and Dirac introduced the Heisenberg spin chain [53,54]. It is a quantum mechanics-based model for investigating the ferromagnetic and anti-ferromagnetic properties of matter, particularly when the interactions between the spins can lead to collective behaviors with macroscopic results, such as ferromagnetism, where neighboring spins line up parallel to each other, and antiferromagnetism, where neighboring spins point in opposite directions. The source of such spontaneous magnetization is the so-called exchange interaction. We introduce one-dimensional model describing the incorporating system of spin-$\frac{1}{2}$ anisotropic chain and SOI effect with inhomogeneous external magnetic fields. Such a system is described by the following Hamiltonian [42,43]:

$$\hat{H} = \sum_{k=1}^{N-1}[\sum_{d=x,y,z} J_d \hat{\sigma}_k^d \hat{\sigma}_{k+1}^d + (\Gamma_z + \mathcal{D}_z)\hat{\sigma}_k^x \hat{\sigma}_{k+1}^y + (\Gamma_z - \mathcal{D}_z)\hat{\sigma}_k^y \hat{\sigma}_{k+1}^x] + \sum_{k=1}^{N} M_{zk}\hat{\sigma}_k^z, \tag{1}$$

where N is the number of qubits and $\hat{\sigma}_k^{d=x,y,z}$ represents a Pauli matrix. In Eq. (1), the first term stands for the Heisenberg XYZ chain with the exchange coupling ($J_{d=x,y,z}$) as the anisotropic coupling coefficient and for most of the paper, we assume ($J_d = J$) and nearest neighbor interactions. The present chain is an antiferromagnetic when J_d is larger than zero while is a ferromagnetic when J_d is smaller than zero (i.e., If $J_d > 0$ positive ($J_d < 0$ negative) values are corresponding to AFM (FM) interaction). If $J_x = J_y$ and $= J_z$, we have an XXX Heisenberg model. While the case $J_x = J_y \neq J_z$ represents the XXZ Heisenberg model, our major interest in this work is the case where we have $J_x \neq J_y \neq J_z \neq 0$, symbolizing the XYZ Heisenberg spin chain [55]. The second and third terms are the first and second orders in SOI around the z-axis, with $\mathcal{D}_z$ indicating the DMI strength. This type of exchange occurs in spin systems due to the coupling of the electron to the angular momentum of the positive ion. We also consider the effects of anisotropic antisymmetric spin–orbit interactions. While Γ_z indicates the KSEA traceless tensor strength, represents the symmetric orbit–spin coupling contribution of the KSEA (z–KSEA) interaction, which is most often ignored in several works but may have a particular impact on the dynamical properties of quantum systems. The fourth term represents the inhomogeneous external magnetic fields that perpendicular to the DMI vector with strength (M_z). Here, we suppose that $M_{z1} = \frac{(G+\Delta)}{2}$ and $M_{z2} = \frac{(G-\Delta)}{2}$, where $G\,(\Delta)$ denotes to the amount of homogeneity (inhomogeneity) of the magnetic field.

Now, we consider the case of the two spins interacting (i.e., $N = 2$) in an anisotropic Heisenberg XYZ chain in the existence of the DMI and KSEA along the z-axis, which can be described as;

$$\mathcal{H}_{zz} = \frac{(G+\Delta)}{2}\sigma_1^z + \frac{(G-\Delta)}{2}\sigma_2^z + J_x\sigma_1^x\sigma_2^x + J_y\sigma_1^y\sigma_2^y + J_z\sigma_1^z\sigma_2^z + \\ +(\Gamma_z + \mathcal{D}_z)\hat{\sigma}_1^x\hat{\sigma}_2^y + (\Gamma_z - \mathcal{D}_z)\hat{\sigma}_1^y\hat{\sigma}_2^x \tag{2}$$

For particular values of the parameters of the system, an analytic expression can be determined (see in the Appendix). To describe the spin system in the case of thermodynamic equilibrium at temperature (T), we use the following density operator:

$$\rho^{AB}(T) = \frac{1}{Z}e^{-H/K_\beta T} = \frac{1}{Z}\sum_i e^{-\lambda_i/K_\beta T}|S_i\rangle\langle S_i| \tag{3}$$

where K is the Boltzmann constant and $\mathcal{Z}$ refers to the system partition function. According to the above standard basis and used the eigenvalues and eigenstates, the analytical expression of $\hat{\rho}(T)$ is given by:

$$\hat{\rho}(T) = \frac{1}{\mathcal{Z}}\big[\chi_{11}|00\rangle\langle 00| + \chi_{14}|00\rangle\langle 11| + \chi_{22}|01\rangle\langle 01| + \chi_{23}|01\rangle\langle 10| \\ + \chi_{32}|10\rangle\langle 01| + \chi_{33}|10\rangle\langle 10| + \chi_{41}|11\rangle\langle 00| + \chi_{44}|11\rangle\langle 11|\big], \tag{4}$$

where

$$\chi_{11} = e^{-\beta J_z}\frac{[\alpha_2\cosh(\alpha_2\beta) - G\sinh(\alpha_2\beta)]}{\alpha_2}, \qquad \chi_{22} = e^{\beta J_z}\frac{[\alpha_1\cosh(\alpha_1\beta) - \Delta\sinh(\alpha_1\beta)]}{\alpha_1},$$
$$\chi_{23} = -e^{\beta J_z}\frac{\sinh(\alpha_1\beta)(J_x + J_y + 2i\mathcal{D}_z)}{\alpha_1}, \qquad \chi_{14} = e^{-\beta J_z}\frac{\sinh(\alpha_2\beta)(-J_x + J_y + 2i\Gamma_z)}{\alpha_2},$$
$$\chi_{33} = e^{\beta J_z}\frac{[\alpha_1\cosh(\alpha_1\beta) + \Delta\sinh(\alpha_1\beta)]}{\alpha_1}, \qquad \chi_{44} = e^{-\beta J_z}\frac{[\alpha_2\cosh(\alpha_2\beta) + G\sinh(\alpha_2\beta)]}{\alpha_2},$$

$\chi_{41} = \chi_{14}^*$, $\chi_{32} = \chi_{23}^*$, $\beta = \frac{1}{KT}$, and $\mathcal{Z} = 2[e^{-\beta J_z}\cosh(\alpha_2\beta) + e^{\beta J_z}\cosh(\alpha_1\beta)]$. In what follows, the thermal non-classical correlations of two coupling spins will be quantified and studied against the above parameters, with the main focus on J_z and Γ_z.

Nonclassical correlation measures

In the following context, we utilize some measures like the local quantum uncertainty, Bell non-locality and entanglement concurrence to investigate the thermal equilibrium correlations of the two-spin information resources.

Basic concepts of measures

- Local quantum uncertainty
  We start with the local quantum uncertainty measure (i.e., L) [25] that determines the minimal uncertainty associated to a single measurement observable on the subsystem. So, for the thermal correlation of the two coupling spins, we can obtain analytical expression of closed form of L for any dimension of bipartite system as follows:

  $$L(T) = 1 - \max\{\Lambda_1, \Lambda_2, \Lambda_3\} \tag{5}$$

  where $\Lambda_r (r = 1,2,3)$ refers to the eigenvalues of symmetric correlation matrix W_{ab} with dimension 3×3 (see Appendix). The elements of ω_{ab} are given by:

  $$(\omega_{ab})_{ks} = \mathrm{Tr}\{\sqrt{\hat{\rho}(T)}(\hat{\sigma}_k\otimes I)\sqrt{\hat{\rho}(T)}(\hat{\sigma}_s\otimes I)\} \tag{6}$$

  with $(k,s = x,y,z)$, $\hat{\sigma}$'s represent the Pauli matrices, and I is an 2×2 identity matrix.
- Bell nonlocality
  According to [11,56], the indicator of two-spin Bell non-locality (i.e., B) can be specified by the maximal values of the two-spin Bell function. The two-spin Bell function can be analytically given by:

  $$B(T) = 2\sqrt{R_\rho(T)} = 2\sqrt{\max_{i<j}(u_i + u_j)} \tag{7}$$

  where $u_{i,j}\,(i,j = 1,2,3)$ indicates the two largest eigenvalues of $\hat{\rho}(T)$ and its amount is less than one (see Appendix). Here, this quantity R_ρ can be employed to determine the violation degree of B. So, when $R_\rho > 1$, then $B > 2$ and causing violation of B. This means that the states have nonlocal correlation. In another aspect, to specify the violation of Bell inequality, the maximal Bell function is given by the form:

  $$B(T) = \sqrt{\max[0, R_\rho(T) - 1]}. \tag{8}$$

  For R_ρ, we find that $0 \le B \le 1$, such that $B = 1$ signifies the largest inequality violation. One can observe that for increasing the degree of B above zero, the violation of B also gradually increasing.
- Entanglement concurrence
  In order to describe the dynamic evolution of quantum entanglement we use Wootters' concurrence [57]. For any two qubits, the concurrence may be calculated explicitly from their density matrix ρ for qubits A and B as:

  $$C(\rho) = \max\left\{0, \sqrt{\tau_1} - \sqrt{\tau_2} - \sqrt{\tau_3} - \sqrt{\tau_4}\right\},$$

  where the quantities τ_i are the eigenvalues in decreasing order of the matrix ζ :

  $$\zeta = \rho\left(\sigma_y\otimes\sigma_y\right)\rho^*\left(\sigma_y\otimes\sigma_y\right),$$

  where ρ^* denotes the complex conjugation of ρ in the standard basis $|0,n\rangle, |1,m\rangle, n,m = 0,1$ and σ_y is the Pauli matrix . The expression of the concurrence of an arbitrary X state was found in Ref. [57] (i.e., C) was considered a most common measure to investigate the entanglement between the two-spin. The analytical expression for this measure is given by:

  $$C(T) = 2\max\left\{0, C_1(T), C_2(T)\right\}, \tag{9}$$

  where $C_1(T) = \sqrt{\rho_{14}\rho_{41}} - \sqrt{\rho_{22}\rho_{33}}$, $C_2(T) = \sqrt{\rho_{23}\rho_{32}} - \sqrt{\rho_{11}\rho_{44}}$, and $\rho_{rj}\,(r,j = 1,\dots,4)$ refers to the matrix elements of density operator. One can observe that for the maximally entangled states C is equal unity and for the separable states C vanishes.

Results and discussion

In this part, we examine the thermal nonclassical correlations (TNC) by using the local quantum uncertainty (Dashed curve), entanglement concurrence (Solid curve) and Bell non-locality (Dot dashed curve) for the bipartite system spins under the effects of KSEA and DMI.

Fig. 1(a), (b) display the TNC measures (i.e, C, L and B) as a function of KT. We observe that the uncertainty of TNC are decreasing with the increasing of temperature. Also, with KT near to zero, the curves of C, L, and B are close to one, and they begin to drop after approaching a specific temperature. Furthermore, by raising the value of Γ_z, the temperature at which TNC begins to decline will increase. This means that, the degree of TNC in the proposed system is enhanced, see Fig. 1(a), (b). Also, the L and C curves dies out exponential by increasing the temperature whereas happens a sudden death of B prior the other curves. In this regard, the L and C measures are more robust than B, and it is difficult to maintain the Bell function when KT approaches to infinity. It is worth noting that the thermodynamic quantum correlation grows stronger as Γ_z strength increases, and the local quantum uncertainty will preserve correlations even if the system is uncorrelated. Furthermore, the Bell non-locality and concurrent entanglement vanish for a specific limiting value of T, which grows with rising Γ_z parameter values. As a result, Bell non-locality [45], may be observed in the considering system, as well as an entangled–unentangled phase transition with Γ_z-dependent critical temperature.

In Fig. 1(c), (e), (d) and (f), we explore the dynamic behavior of the thermal correlation against the KSEA effect for different values of

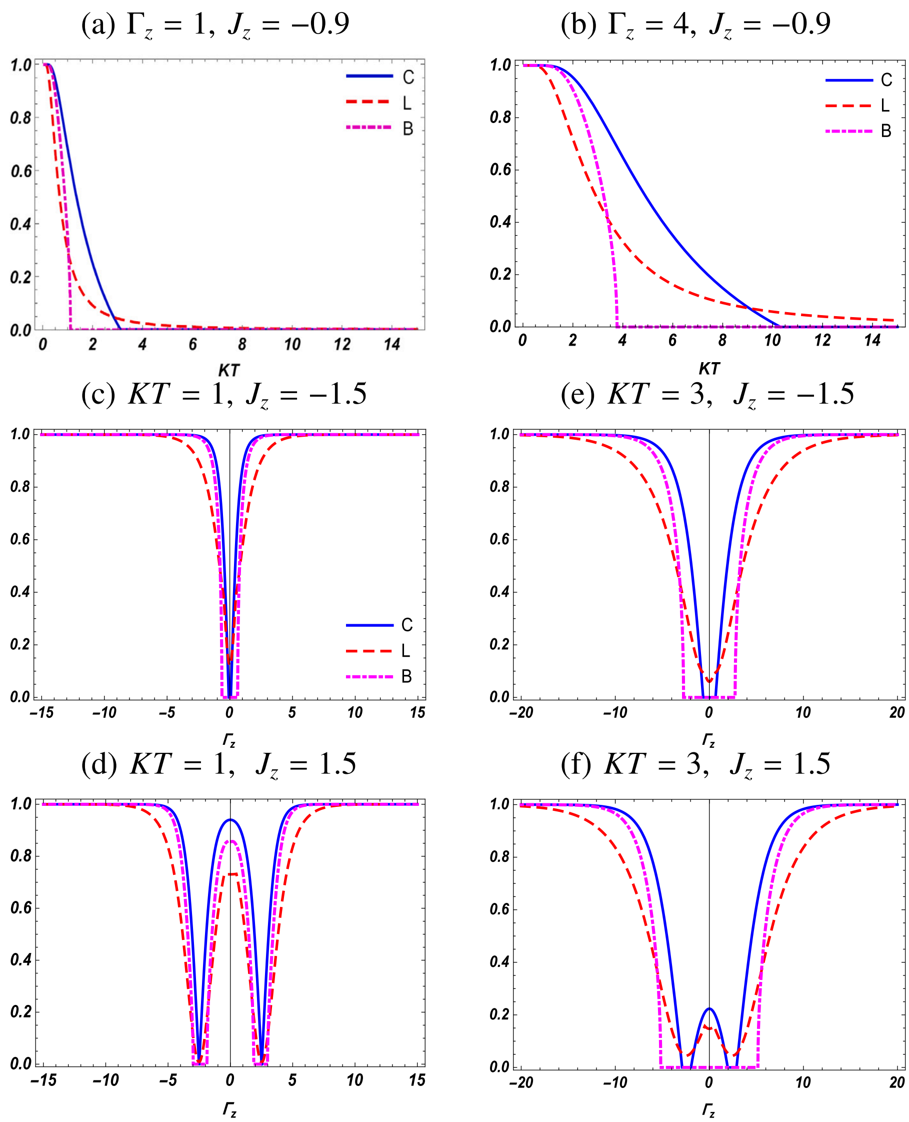

Fig. 1. TNC behavior against the temperature and KSEA effect, with $J_x = 0.2$, $J_y = 0.1$, $G = 0.05$, $\Delta = 0$, and $D_z = 1$.

the equilibrium temperature and the coupling constant between two neighboring qubits J_z. From Fig. 1(c), (e), when (T = 1,3) and $J_z = -1.5$, the behavior of C, L and B measures are symmetric functions about $\Gamma_z = 0$ regardless of the uniform magnetic field ratios. It is find that the increase of spin–orbit interaction $|\Gamma_z|$ enhances the correlations. It is clear in Fig. 1(c) that when Γz disappears, the C, L, and B attain their minimum and maximum values, respectively Fig. 1(e). Also, we discover that the Bell nonlocality vanishes for a specific limiting value of T before the concurrence entanglement, and it is influenced by an increase in temperature that causes sudden death, while the L remains nonzero. This means that the Bell nonlocality is more sensitive to Γ_z than other measures. Besides, for in the absence of KSEA, we observe from Fig. 1(e) that the Bell inequality is not violated and that a local correlation may be established despite the absence of bipartite entanglement. By increasing KSEA by a sufficient amount the B violation occurs and the dynamics of L approach the minimal value without reaching zero. For the correlations between quantum systems description, L is more adapted than B and C. Fig. 1(d)–(f), depicts the behavior of the QCs curves under identical conditions to Fig. 1(a), but with $J_z = 1.5$ and $T = (1, 3)$, respectively. It is noted that the thermal concurrence entanglement has the maximal value in the region around $\Gamma_z = 0$ other than both B and L. Moreover, for constant temperature values, we observe from Fig. 1(e), (f) that the thermal correlations are suppressed by a small fraction of $|\Gamma_z|$. Remarkably, in Fig. 1(f) the area of the window in which the B inequality is not violated is larger than in Fig. 1(d). Eventually, when KSEA becomes more stronger the non-local correlations occur less. This indicates that L can capture quantum correlations when antiferromagnetic coupling $J_z > 0$ or ferromagnetic coupling $J_z < 0$ under the KSEA effect for increasing temperature, i.e., (L is more robust against temperature.) All these results show that quantum non locality and entanglement are not the same as quantum correlations. Quantum non locality and entanglement are only a special kind of quantum correlations.

Fig. 2 shows the impact of the constant exchange coefficient J_z on TNC. In Fig. 2(a)–(d), it is noted that the amount of TNC grows as the value of J_z increases reaching a constant maximum for both ferromagnetic ($J_z < 0$) and antiferromagnetic ($J_z > 0$) regions. At critical value of J_z, one can observe that B and C vanish whereas local uncertainty will persists. This implies that L can identify the critical regions of quantum phase change at a finite temperature whereas B and C cannot. In addition, we note that correlations undergo an abrupt change at critical points for only antiferromagnetic region. Besides, at low temperature, the TNC frequently exhibits similar behaviors, see Fig. 2(a), (b). With rising temperature, both C and B decline and L decreases asymptotically, and then they stabilize to a near-stable value, with C being bigger than B and L as exchange coupling increases. The

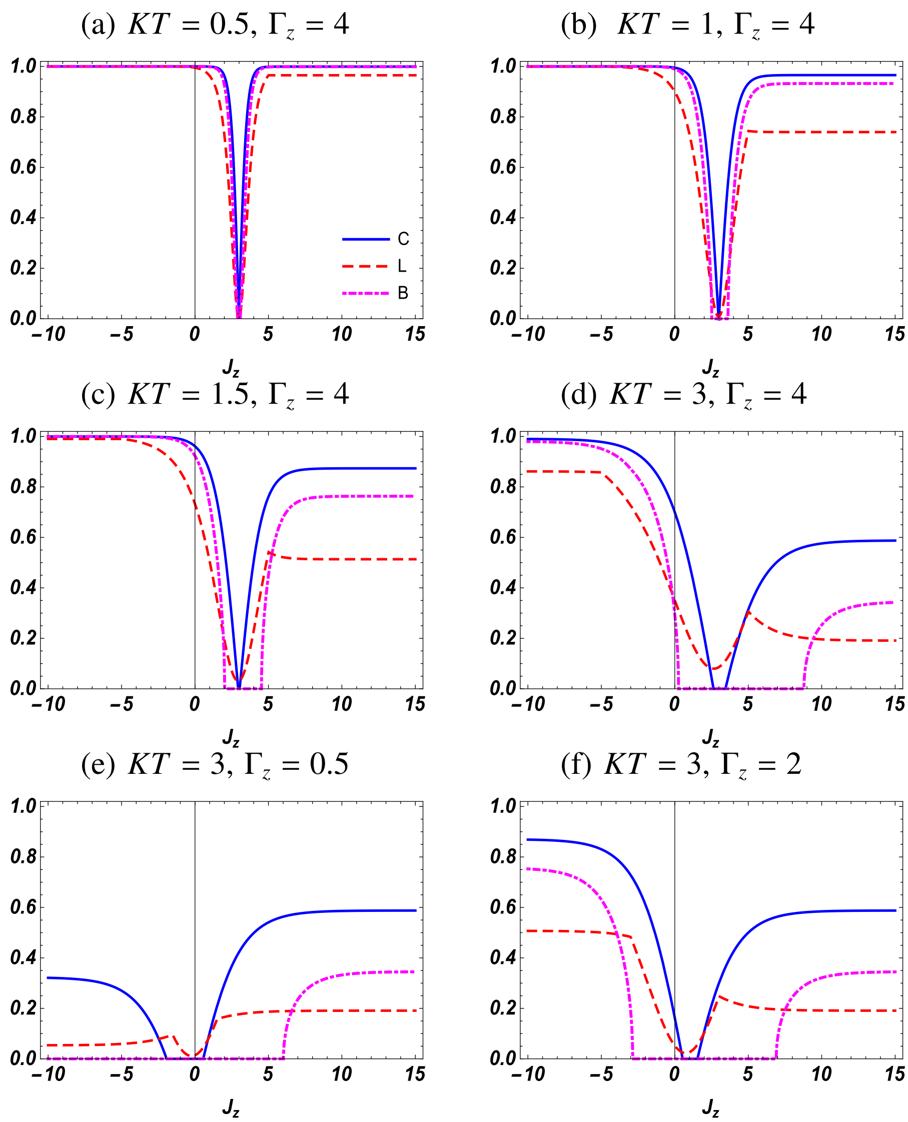

Fig. 2. TNC behavior versus the exchange coupling impact, with $J_x = 0.2$, $J_y = 0.1$, $G = 0.05$, $\Delta = 0$, and $D_z = 1$.

correlations of the quantitative curves, on the other hand, behave identically in both regions and remain significantly present in the region where $J_z < 0$ even at higher temperatures, as illustrated in Fig. 2(c), (d). Furthermore, when temperature increases, the correlations in the region of $J_z > 0$ changes abruptly. Finally, we may expect SOI around the z-axis to establish conditions that protect and preserve the value of thermal correlations in the current system with low temperature. Furthermore, thermal local quantum uncertainty is more resistant to temperature than thermal entanglement. It is worth noting that the pairwise thermal correlation L exhibits quantum correlations even when the concurrence is zero and the Bell nonlocality is present. This demonstrates that L can reveal quantum correlations that neither C nor B can capture.

Fig. 2(e), (f), illustrate the features of correlations as a function of J_z for various values of Γ_z. As shown in Fig. 2(e), C and L do not vanish in the neighborhood of $J_z < 0$ and $\Gamma_z < 0.5$, however violations of B can never happen. We can see from Fig. 2(f) that there is a dramatic shift in C and L, whereas B is no longer equal to zero as the negative J_z interaction increases. Furthermore, when J_z increases, the thermal C, L, and B reach an unified steady-state that remains constant at finite temperature. It is worth noting that the revival of C, L, and B inside the ferromagnetic range is dependent on an increase in the value of Γ_z at a constant temperature, whereas they are stable and have a nearly unchanged value at a fixed temperature regardless of the value of Γ_z in the antiferromagnetic region.

Fig. 3 displays the effect of J_y coupling on the thermal correlation of the two-spin system. From Fig. 3(a), we note that the quantities of thermodynamic quantum correlations are weakened for both ferromagnetic and antiferromagnetic cases. We observe that the TNC curves reach their highest value in the crucial band and fall to the least amount in the antiferromagnetic zone than in the ferromagnetic region, as shown in Fig. 3(b), (d). Furthermore, when J_x increases, the amount of correlations in the ferromagnetic region increases more than in the antiferromagnetic region, and they do not appear at critical values of J_y, see Fig. 3(c). However, given a strong effect of KSEA and exchange coupling J_x, we estimate that the amount of TNC has a stronger effect on the system and less information is lost.

Fig. 4, depicts the dynamic of a TNC in the presence of a magnetic field. It is worth noting that thermal correlations based on inhomogeneity of the magnetic field will be significant due to the robust effect of DMI and the weak effect of KSEA, and vice versa. Also, it finds that the lower bound of such quantifiers diminishes as the magnetic value goes up. From Fig. 4(a), (b), we can find that the B nonlocality is more sensitive to these effects compared to C and L. Besides, from Fig. 4(c), (d), one can note both C, L and B are symmetric for the external magnetic field and B nonlocality does not vanish compared

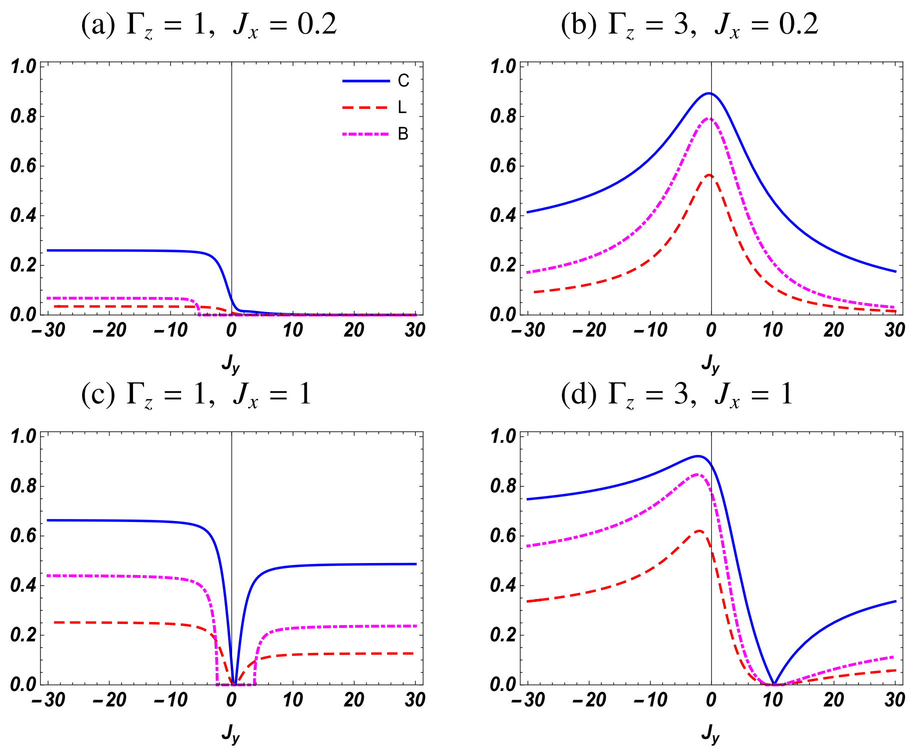

Fig. 3. TNC behavior versus the effect of J_y, with $J_z = 0.2$, $KT = 1.5$, $G = 0.05$, $\Delta = 0$ and $\mathcal{D}_z = 1$.

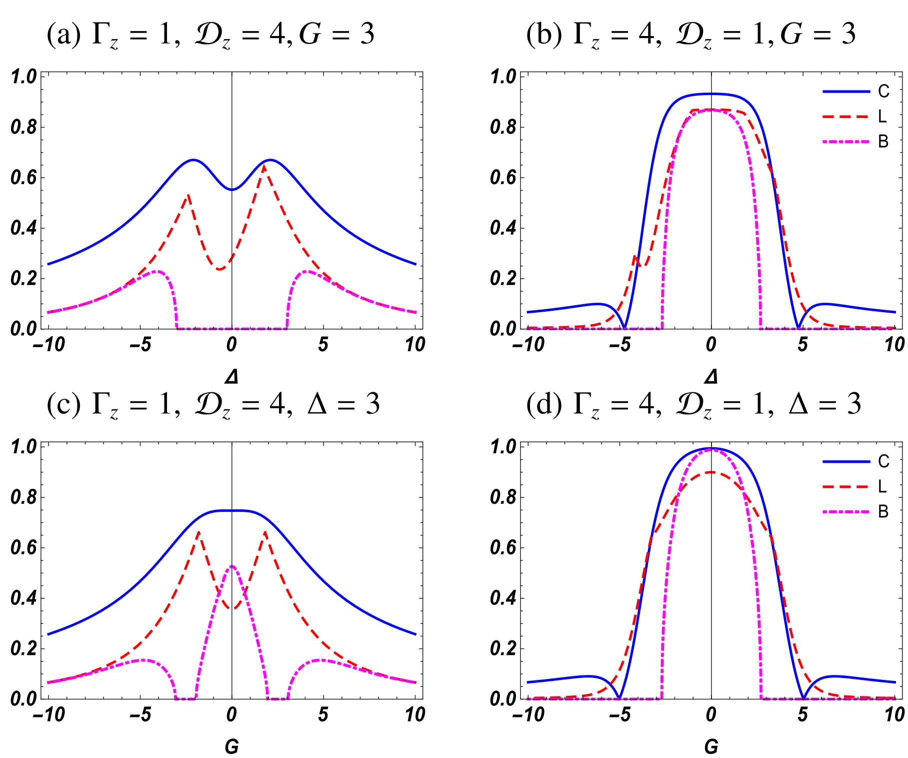

Fig. 4. Impact of homogeneity and inhomogeneity of magnetic field on TNC, with $J_x = 0.2$, $J_y = 0.1$, $J_z = -1.5$ and $KT = 1.5$.

to Fig. 4(a). In addition, the thermal correlations of Fig. 4(c), (d) are stronger than the case of inhomogeneity magnetic field. However, at zero homogeneity (or inhomogeneity) magnetic field that the SOI effect can enhance the strength of TNC, causing that C realizes its greatest amount and becomes more stable than B and L.

Conclusions

We have explored the thermodynamic evolution of the quantum correlations for a two-qubit system modeled by an XYZ Heisenberg chain with an external magnetic field and considering KSEA and DMI effects.

For a two-qubit system modeled by an XYZ Heisenberg chain with an external magnetic field and both KSEA and DMI effects, we investigated the thermodynamic development of the features of the systemic quantum correlations bound. First, we have computed the eigenvalues and eigenvectors for a two-qubit quantum system analytically, and then we have estimated the thermal equilibrium state at a finite temperature. The local quantum uncertainty, Bell inequality, and concurrence for the Heisenberg XYZ model under physical parameters are determined analytically. We have proven that the thermal temperature reduces the non-classical correlations of the quantum system, resulting in the destruction of the correlations in the system. Furthermore, stronger exchange coupling lowers non-classical correlations in an antiferromagnetic case, but enhances them in a ferromagnetic case. The effect of DMI-KSEA interactions on the FM and AFM phases are investigated using coupling constants of various absolute temperatures. Moreover, we have explored the three measures mentioned above in terms of coupling constants and for different temperature.

Our results reveal that the created two-spin correlations achieve their maximum levels at relatively low temperatures and do not begin to dissolve until a threshold temperature has been reached. However, we have shown that the KSEA effect is directly connected to the emergence of the effect of temperature fluctuations, which destroys the quantum correlation system's coherence. Furthermore, the Local quantum uncertainty reveals and identifies non-classical correlations in the 2-spin XYZ Heisenberg ferromagnetic (antiferromagnetic) quantum system as the temperature increases. We find that the Bell nonlocality vanishes for a particular small amount of the temperature before the concurrence, and it is affected by a temperature increase that causes sudden death, while the local quantum uncertainty does not vanish. The KSEA interactions suppress the local minimum of the local quantum uncertainty. Our results indicate that the strength of the symmetry parameters KSEA with the magnetic fields yields a more efficient quantum correlation than the antisymmetric control strength DMI. The symmetric KSEA may protect and eventually enhance the amount of quantum correlations in the system. Moreover, it contributes to reduce the destructive effects of the thermal fluctuations. Finally, we predict that a more efficient quantum correlation can be obtained under the strength increase of KSEA compared to the DMI.

CRediT authorship contribution statement

Ahmad N. Khedr: Conceptualization, Formal analysis, Investigation, Methodology, Software, Validation, Visualization, Writing – original draft, Writing – review & editing. **Ali H. Homid:** Conceptualization, Formal analysis, Investigation, Methodology, Validation, Visualization, Writing – original draft, Writing – review & editing. **Abdel-Baset A. Mohamed:** Conceptualization, Formal analysis, Investigation, Methodology, Validation, Visualization, Writing – original draft, Writing – review & editing. **Abdel-Haleem Abdel-Aty:** Conceptualization, Formal analysis, Investigation, Software, Validation, Visualization, Writing – original draft, Writing – review & editing. **Hichem Eleuch:** Conceptualization, Investigation, Methodology, Validation, Writing – original draft, Writing – review & editing. **Mahmoud Tammam:** Conceptualization, Formal analysis, Investigation, Software, Validation, Writing – original draft, Writing – review & editing. **Mahmoud Abdel-Aty:** Conceptualization, Formal analysis, Investigation, Validation, Visualization, Writing – original draft, Writing – review & editing.

Declaration of competing interest

The authors declare that they have no known competing financial interests or personal relationships that could have appeared to influence the work reported in this paper.

Appendix

We give the eigenvalues and the corresponding eigenstates of Hamiltonian in Eq. (2) in terms of the standard basis $H(|0,n\rangle, |1,m\rangle, n, m = 0, 1)$. By using the condition of the eigenvalue-problem:

$\hat{H}|S_i\rangle = \lambda_i|S_i\rangle (i = 1, 2, 3, 4)$

Hence, the energy spectrum across the eigenvalues (i.e., λ_k) are calculated as follows:

$\lambda_1 = -J_z - \alpha_1, \lambda_2 = -J_z + \alpha_1, \lambda_3 = J_z - \alpha_2, \lambda_4 = J_z + \alpha_2,$

$\alpha_1 = \sqrt{(J_x + J_y)^2 + \Delta^2 + 4D_z^2}$, $\alpha_2 = \sqrt{(J_x - J_y)^2 + G^2 + 4\Gamma_z^2}$, the corresponding eigenvectors (i.e., $|S_j\rangle$) can be written as:

$$\begin{pmatrix} |S_1\rangle \\ |S_2\rangle \\ |S_3\rangle \\ |S_4\rangle \end{pmatrix} = M \begin{pmatrix} |0,n\rangle \\ |0,n\rangle \\ |1,m\rangle \\ |1,m\rangle \end{pmatrix}, M = \begin{pmatrix} \frac{\eta_{j_1}}{\sqrt{|\eta_{j1}|^2+1}} & 0 & 0 & \frac{\eta_{j_1}}{\sqrt{|\eta_{j1}|^2+1}} \\ 0 & \frac{\eta_j}{\sqrt{|\eta_j|^2+1}} & \frac{\eta_j}{\sqrt{|\eta_j|^2+1}} & 0 \\ 0 & \frac{1}{\sqrt{|\eta_j|^2+1}} & \frac{1}{\sqrt{|\eta_j|^2+1}} & 0 \\ \frac{1}{\sqrt{|\eta_{j1}|^2+1}} & 0 & 0 & \frac{1}{\sqrt{|\eta_{j1}|^2+1}} \end{pmatrix} \tag{10}$$

$\eta_j = \frac{(-1)^j \alpha_1 + \Delta}{J_x + J_y - 2iD_z}$, $\eta_{j_1} = \frac{(-1)^{j_1} \alpha_2 + G}{J_x - J_y + 2i\Gamma_z}$, here $i = 1, 2$. Now the density matrix is estimated by the following expression:

$$\rho^{ab}(T) = \frac{1}{Z}[e^{-\lambda_1\beta}|S_1\rangle\langle S_1| + e^{-\lambda_2\beta}|S_2\rangle\langle S_2| + e^{-\lambda_3\beta}|S_3\rangle\langle S_3| + e^{-\lambda_4\beta}|S_4\rangle\langle S_4|] \tag{11}$$

where the partition function is defined $Z = e^{-\beta\lambda_1} + e^{-\beta\lambda_2} + e^{-\beta\lambda_3} + e^{-\beta\lambda_4}$.

Now, we analytically present the local quantum uncertainty and maximum violation of Bell–CHSH inequality for a more general class of two-qubit states, X-structured states in Eq. (4), which are represented in the orthonormal basis $|0,n\rangle$ and $|1,n\rangle$ where $n = 0, 1$.

Local Quantum Uncertainty To calculate the analytical expression of the local quantum uncertainty based on skew information, using local unitary operations, the phase factors (off-diagonal elements) can be disposed of via a convenient local unitary transformation $U_a \otimes U_b$. All non-classical correlations and quantum entanglement remain constant under the local unitary transformations. Let us first consider the following local unitary transformations

$$\rho_X^{ab} \rightarrow \grave{\rho}_X^{ab} = (U_a \otimes U_b)\rho_X^{ab}(U_a \otimes U_b)^\dagger \tag{12}$$

where, $U_a \rightarrow \exp(\frac{-i}{2}(\vartheta_{14} + \vartheta_{23}))|0\rangle_a$, $U_b \rightarrow (\exp(\frac{-i}{2}(\vartheta_{14} - \vartheta_{23})|0\rangle_b))$. We obtain density state:

$$\rho_X^{ab} = \begin{pmatrix} \chi_{11} & 0 & 0 & |\chi_{14}| \\ 0 & \chi_{22} & |\chi_{23}| & 0 \\ 0 & |\chi_{32}| & \chi_{33} & 0 \\ |\chi_{41}| & 0 & 0 & \chi_{44} \end{pmatrix} \tag{13}$$

This process does not affect the value of non-classical correlations in the system. The Fano-Bloch degeneration of the state $\grave{\rho}_X^{ab}$ can be written as:

$$\grave{\rho}_X^{ab} = \frac{1}{4}(\sum_{\alpha,\beta} \mathcal{R}_{\alpha\beta}\vec{\sigma}_\alpha \otimes \vec{\sigma}_\beta) \tag{14}$$

where σ_0 is identity matrices, $\{\sigma\}_{i=1}^3$ are the basis Pauli operator and the correlation matrix $\mathcal{R}_{\alpha,\beta}$ are given by $\mathcal{R}_{\alpha,\beta} = Tr(\grave{\rho}_X^{ab}\vec{\sigma}_\alpha \otimes \vec{\sigma}_\beta)$ with $(\alpha, \beta = 0, 1, 2, 3)$.

For the density matrix in Eq. (13), the non vanishing correlation matrix terms for this system are:

$\mathcal{R}_{0,0} = K_{11} + K_{22} + K_{33} + K_{44} = 1, \mathcal{R}_{1,1} = 2(|K_{23}| + |K_{14}|),$

$\mathcal{R}_{2,2} = 2(|K_{23}| - |K_{14}|), \mathcal{R}_{3,3} = 1 - 2(K_{22} + K_{33}),$

$\mathcal{R}_{0,3} = 2(K_{11} + K_{33}) - 1, \mathcal{R}_{3,0} = 2(K_{11} + K_{22}) - 1.$

Using the following relations of the Pauli matrices

$$\{\sigma_i,\sigma_j\} = 2\delta_{ij}, \quad Tr\left(\sigma_i\sigma_j\right) = 2\delta_{ij},$$
$$Tr\left(\sigma_i\sigma_j\sigma_k\sigma_l\right) = 2\left(\delta_{ij}\delta_{kl} - \delta_{ik}\delta_{jl} + \delta_{il}\delta_{jk}\right) \tag{15}$$

Similarly, we can obtain the Fano-Bloch decomposition of matrix $\sqrt{\rho^{ab}{}_X}$ with $\mathcal{R}_{\alpha,\beta} = Tr(\sqrt{\grave{\rho}^{ab}{}_X}\vec{\sigma}_\alpha \otimes \vec{\sigma}_\beta)$ as

$$\sqrt{\grave{\rho}^{ab}{}_X} = \frac{1}{4}\sum_{\alpha,\beta}\mathcal{R}_{\alpha,\beta}\sigma_\alpha \otimes \sigma_\beta \tag{16}$$

According to Eq: (6), we can determine matrix W where the diagonal elements and off-diagonal elements are $w_{ii} = \frac{1}{4}\left[\sum_\beta\left(\mathcal{R}^2_{0\beta} - \sum_k \mathcal{R}^2_{k\beta}\right)\right] + \frac{1}{2}\sum_\beta \mathcal{R}^2_{i\beta}(\beta = 0,1,2,3),(i,k) = 1,2,3$ and $w_{ij} = \frac{1}{2}\mathcal{R}_{i\beta}\mathcal{R}_{j\beta}$ $(i \neq j)$, respectively. It can be easily expressions of the elements w_{ij} involve only the nonvanishing Fano-Bloch components of the square root of the density matrix given by:

$$w_{11} = \frac{1}{4}\left(\left(\mathcal{R}^2_{1,2} - \mathcal{R}^2_{2,1}\right) + \left(\mathcal{R}^2_{1,1} - \mathcal{R}^2_{2,2}\right) + \left(\mathcal{R}^2_{0,3} - \mathcal{R}^2_{3,0}\right) + \left(\mathcal{R}^2_{0,0} - \mathcal{R}^2_{3,3}\right)\right)$$

$$w_{22} = \frac{1}{4}\left(\left(\mathcal{R}^2_{2,2} - \mathcal{R}^2_{1,1}\right) + \left(\mathcal{R}^2_{2,1} - \mathcal{R}^2_{1,2}\right) + \left(\mathcal{R}^2_{0,3} - \mathcal{R}^2_{3,0}\right) + \left(\mathcal{R}^2_{0,0} - \mathcal{R}^2_{3,3}\right)\right)$$

$$w_{33} = \frac{1}{4}\left(-\left(\mathcal{R}^2_{1,2} + \mathcal{R}^2_{2,1}\right) - \left(\mathcal{R}^2_{1,1} + \mathcal{R}^2_{2,2}\right) + \left(\mathcal{R}^2_{0,3} + \mathcal{R}^2_{3,0}\right) + \left(\mathcal{R}^2_{0,0} + \mathcal{R}^2_{3,3}\right)\right)$$

$$w_{12} = w_{21} = \frac{1}{2}(\mathcal{R}_{1,1}\mathcal{R}_{2,1} + \mathcal{R}_{1,2}\mathcal{R}_{2,2}) \quad w_{13} = w_{31} = 0 \quad and$$
$$w_{23} = w_{32} = 0$$

Consecutively, we can obtain the eigenvalues of Λ_i of the matrix $\mathbf{W_{AB}}$ Eq. (5) as

$$\Lambda_1 = \frac{1}{2}\left(w_{11} + w_{22} + \sqrt{(w_{11} - w_{22})^2 + 4w^2_{12}}\right) \tag{17}$$

$$\Lambda_2 = \frac{1}{2}\left(w_{11} + w_{22} - \sqrt{(w_{11} - w_{22})^2 + 4w^2_{12}}\right) \tag{18}$$

$$\Lambda_3 = w_{33} \tag{19}$$

Accordingly, using this, we calculate LQU from Eq. (6) for the state $\rho(T)$. We see that LQU appreciates numerous remarkable properties. It is constant under any local unitary operations, and it evolves to zero for product state $\rho_{AB} = \rho_A \otimes \rho_B$. Besides, the LQU is non-increasing (contractive) under local operation on the unmeasured subsystem B.

Bell nonlocality For two-qubit states and X-structured states Eq. (4). Alternatively, the X-shape states can be represented in the Bloch representation as

$$\rho^{ab}_X = \frac{1}{4}(I \otimes I + \sum_{\alpha,\beta=1}^{3} T_{\alpha\beta}\vec{\sigma}_\alpha \otimes \vec{\sigma}_\beta) \tag{20}$$

Here, the termes $T_{\alpha,\beta}$, which are represented by elements $t_{ij} = Tr(\rho^{ab}_X\sigma_i \otimes \sigma_j)$, $\sigma_{1,2,3}$(Pauli spin matrix), are the matrix coefficients of the correlation density matrix $T_{\alpha\beta}$.

In the case of a two-qubit interaction system in the presence of the DMI strength and KSEA strength, the matrix $C = T^t T$ is

$$C = \begin{pmatrix} A_{11} & A_{12} & 0 \\ A_{21} & A_{22} & 0 \\ 0 & 0 & A_{33} \end{pmatrix} \tag{21}$$

The eigenvalues of the matrix C can be derived analytically as follows:

$$u_1 = \frac{1}{2}(A_{11} + A_{22} - \Theta), u_2 = \frac{1}{2}(A_{11} + A_{22} + \Theta), u_3 = A_{33}$$

where $\Theta = \sqrt{(A_{11} - A_{22})^2 + 4A_{12}A_{21}}, A_{11} = t^2_{11} + t^2_{12}, \quad A_{22} = t^2_{21} + t^2_{22}, \quad A_{33} = t^2_{33}, \quad A_{12} = A_{21} = t_{11}t_{21} + t_{12}t_{22}$. Eq. (8) allows us to calculate easily the expression of the quantity $R(\rho)$ such that

$$R(\rho) = \max\left\{u^2_1 + u^2_2, u^2_1 + u^2_3, u^2_2 + u^2_3\right\}$$

Then, we can give the expression of non-locality quantum test Eq. (9) by

$$\mathcal{B}(\rho) = 2\sqrt{\max[0, R(\rho) - 1]} \leq 1.$$

References

[1] Bennett CH, DiVincenzo DP. Quantum information and computation. Nature 2000;404:247–55.
[2] Abliz A, Gao HJ, Xie XC, Wu YS, Liu WM. Entanglement control in an anisotropic two-qubit Heisenberg XYZ model with external magnetic fields. Phys Rev A 2006;74:052105.
[3] Abdel-Aty A, Khedr AN, Saddeek YB, Youssef AA. Thermal entanglement in quantum annealing processor. Int J Quantum Inf 2018;16:1850006.
[4] Mohamed A-BA, Eleuch H. Generation and robustness of bipartite non-classical correlations in two nonlinear microcavities coupled by an optical fiber. J Opt Soc Amer B 2018;35:47.
[5] Einstein A, Podolsky B, Rosen N. Can quantum-mechanical description of physical reality be considered complete? Phys Rev 1935;47:777.
[6] Bell JS. On the Einstein Podolsky Rosen paradox. Physics 1964;1:195.
[7] Khedr AN, Mohamed A-BA, Abdel-Aty A, Tammam M, Abdel-Aty M, Eleuch H. Entropic uncertainty for two coupled dipole spins using quantum memory under the Dzyaloshinskii–Moriya interaction. Entropy 2021;23:1595.
[8] Hensen B, et al. Experimental loophole-free violation of a bell inequality using entangled electron spins separated by 1.3 km. Nature 2015;526:682.
[9] Giustina M, et al. Significant-loophole-free test of Bell's theorem with entangled photons. Phys Rev Lett 2015;115:250401.
[10] Shalm LK, et al. Strong loophole-free test of local realism. Phys Rev Lett 2015;115:250402.
[11] Clauser JF, Horne MA, Shimony A. Holt RA. Proposed experiment to test local hidden-variable theories. Phys Rev Lett 1969;23:880.
[12] Hu M-L, Fan H. Quantum-memory-assisted entropic uncertainty principle, teleportation, and entanglement witness in structured reservoirs. Phys Rev A 2012;86:032338.
[13] Bennett CH, Wiesner SJ. Communication via one- and two-particle operators on Einstein–Podolsky–Rosen states. Phys Rev Lett 1992;69:2881.
[14] Ekert AK. Quantum cryptography based on Bell's theorem. Phys Rev Lett 1991;67:661.
[15] Bennett CH, Brassard G, Mermin ND. Quantum cryptography without Bell's theorem. Phys Rev Lett 1992;68:557.
[16] Pan J-W, Bouwmeester D, Weinfurter H, Zeilinger A. Experimental entanglement swapping: Entangling photons that never interacted. Phys Rev Lett 1998;80:3891.
[17] Bennett CH, Brassard G. Quantum cryptography: Public key distribution and coin tossing. Theor Comput Sci 2014;560:7.
[18] Kimble HJ. The quantum internet. Nature 2008;453:1023.
[19] Pozas-Kerstjens A, Gisin N, Renou MO. Proofs of network quantum nonlocality aided by machine learning. arXiv:2203.16543.
[20] Colbeck R. Quantum and relativistic protocols for secure multi-party computation. arXiv:0911.3814 [quant-ph].
[21] Ollivier H, Zurek WH. Quantum discord: A measure of the quantumness of correlations. Phys Rev Lett 2001;88:017901;
Henderson L, Vedral V. Classical quantum and total correlations. J Phys A 2001;34:6899.
[22] Datta A, Shaji A, Caves CM. Quantum discord and the power of one qubit. Phys Lett Lett 2008;100:050502.
[23] Modi K, Brodutch A, Cable H, Paterek T, Vedral V. The classical-quantum boundary for correlations: Discord and related measures. Rev Modern Phys 2012;84:1655.
[24] Huang Y. Computing quantum discord is NP-complete. New J Phys 2014;16:033027.
[25] Girolami D, Tufarelli T, Adesso G. Characterizing nonclassical correlations via local quantum uncertainty. Phys Rev Lett 2013;110:240402.
[26] Wigner EP, Yanase MM. Part I: Particles and fields. Part II: Foundations of quantum mechanics, Springer; 1997, p. 452–60.
[27] Slaoui A, Daoud M, Laamara RA. The dynamics of local quantum uncertainty and trace distance discord for two-qubit X states under decoherence: a comparative study. Quantum Inf Process 2018;17:1–24.
[28] Jebli L, Benzimoun B, Daoud M. Quantum correlations for two-qubit x states through the local quantum uncertainty. Int J Quantum Inf 2017;15:1750001.
[29] Faizi E, Ahansaz BJ Korean. Local quantum uncertainty of SU(2) invariant states. Phys Soc 2015;67:2033.
[30] Wu S, Zhang Y, Yu C. Local quantum uncertainty guarantees the measurement precision for two coupled two-level systems in non-Markovian environment. Ann Phys 2018;390:71–82.
[31] Yu C, Wu S, Wang X, Yi XX, Song H. Quantum correlation measure in arbitrary bipartite systems. Eur Phys Lett 2014;107:10007.
[32] Kane BE. A silicon-based nuclear spin quantum computer. Nature 1998;133:393.
[33] Fu HC, Dong H, Liu XF, Sun CP. Indirect control with a quantum accessor: Coherent control of multilevel system via a qubit chain. Phys Rev A 2007;75:052317.

[34] Bayat A, Burgarth D, Mancini S, Bayat Bose S, Abolfazl , Burgarth Daniel, Mancini Stefano, Bose Sougato. Memory effects in spin-chain channels for information transmission. Phys Rev A 2008;77:050306.
[35] Sergienko IA, Dagotto E. Role of the dzyaloshinskii-moriya interaction in multiferroic perovskites. Phys Rev B 2006;73:094434.
[36] Vala J, Whaley B. Encoded universality for generalized anisotropic exchange Hamiltonians. Phys Rev A 2002;66:022304.
[37] Abdel-Aty A, Khedr AN, Youssef AA, Saddeek YB. Entanglement of thermal state of quantum annealing processor. Therm Sci 2020;24:325.
[38] Bloch I. Quantum coherence and entanglement with ultracold atoms in optical lattices. Nature 2008;453:1016–22.
[39] Kloeffel C, Loss DAnnuRev Condens. Prospects for spin-based quantum computing in quantum dots. Matter Phys 2013;4:51–81.
[40] Yin J, et al. Satellite-based entanglement distribution over 1200 kilometers. Science 2017;356:1140–4.
[41] Shahbeigi F, Karimi M, Karimipour V. Simulating of X-states and the two-qubit XYZ heisenberg system on IBM quantum computer. Phys Scr 2022.
[42] Dzyaloshinsky I. A thermodynamic theory of weak ferromagnetism of antiferromagnetics. J Phys Chem Solids 1958;4:241.
[43] Moriya T. New mechanism of anisotropic superexchange interaction. Phys Rev Lett 1960;4:228.
[44] Zheludev A, Maslov S, Tsukada I, Zaliznyak I, Regnault LP, Masuda T, Uchinokura K, Erwin R, Shirane G. Experimental evidence for Kaplan–Shekhtman–Entin-Wohlman–Aharony interactions in $Ba_2CuGe_2O_7$. Phys Rev Lett 1998;81:5410.
[45] Park DK. Thermal entanglement and thermal discord in two-qubit Heisenberg XYZ chain with Dzyaloshinskii–Moriya interactions. Quant Inf Process 2019;18:1–24.
[46] Khedif Y, Daoud M, El HSayouty. Thermal quantum correlations in a two-qubit Heisenberg XXZ spin-$\frac{1}{2}$ chain under an inhomogeneous magnetic field. Phys Scr 2019;94:125106.
[47] Souza AM, Reis MS, Soares-Pinto DO, Oliveira IS, Sarthour RS. Experimental determination of thermal entanglement in spin clusters using magnetic susceptibility measurements. Phys Rev B 2008;77:104402.
[48] Yurischev MA. On the quantum correlations in two-qubit XYZ spin chains with Dzyaloshinsky-Moriya and Kaplan-Shekhtman-Entin-Wohlman-Aharony interactions. Quantum Inf Process 2020;19:336.
[49] Fedorova AV, Yurischev MA. Quantum entanglement in the anisotropic heisenberg model with multicomponent DM and KSEA interactions. Quantum Inf Proc 2021;20:169.
[50] Houça R, Choubabi EB, Bouziani ME, Belouad A, Kamal A. Entanglement in a two-qubit heisenberg XXX chain with x-components of Dzyaloshinskii-Moriya and Kaplan-Shekhtman-Entin-Wohlman-Aharony interactions. 2021, arXiv:2110.08854.
[51] Yurischev MA. On the quantum correlations in two-qubit XYZ spin chains with Dzyaloshinsky–Moriya and Kaplan–Shekhtman–Entin–Wohlman–Aharony interactions. Quantum Inf Proc 2020;19:1–20.
[52] Fa KWen, Zhang X. Exact solution of the Gaudin model with Dzyaloshinsky–Moriya and Kaplan–Shekhtman–Entin–Wohlman–Aharony interactions. Chin Phys B 2021;30:050201.
[53] Mattis DC. The theory of magnetism made simple: An introduction to physical concepts and to some useful mathematical methods. Singapore: World Scientific; 2006.
[54] Nolting W, Ramakanth A. Quantum theory of magnetism. Berlin Heidelberg: Springer; 2009.
[55] Martin T, Giresse TA. Entanglement dynamics of a two-qubit XYZ spin chain under both Dzyaloshinskii-Moriya interaction and time-dependent anisotropic magnetic field. Int J Theor Phys 2020;59:2232–48.
[56] Horodecki R, Horodecki P, Horodecki M. Violating Bell inequality by mixed spin-12 states: necessary and sufficient condition. Phys Lett A 1995;200:340–4.
[57] Wootters WK. Entanglement of formation of an arbitrary state of two qubits. Phys Rev Lett 1998;80:2245.